Eur. Phys. J. B **36**, 411–418 (2003)
DOI: 10.1140/epjb/e2003-00360-7

THE EUROPEAN PHYSICAL JOURNAL B

Size effect of quantum conductance in single-walled carbon nanotube quantum dots

H. Liu[1,2,a] and Y. Tao[1]

[1] Physics Department, Nanjing Normal University, Nanjing 210097, P.R. China
[2] Physics Department, Peking University, Beijing 100871, P.R. China

Received 31 May 2003 / Received in final form 8 August 2003
Published online 23 December 2003 –

Abstract. The quantum conductance of two kinds of carbon nanotube quantum dots (CNQD) composed of (5,5) and (10,0) tubes, namely (10,0)/(5,5)/(10,0) and (5,5)/(10,0)/(5,5) with different quantum sizes, are calculated. It is shown that for (10,0)/(5,5)/(10,0) CNQD, one on-resonant peak at the Fermi energy exists only for special QD sizes, and the width of the conductance gap increases from 1.0 eV to 3.2 eV with the increase of size. The positions of peaks around the Fermi energy are obtained by the electronic structure of individual finite (5,5) tubes. We also find that the (5,5)/(10,0)/(5,5) CNQDs behave as a quantum dot, and its localized QD states are different from that of the former CNQD because of the existence of the interface states between (5,5)/(10,0) junctions. For (5,5)/(10,0)/(5,5) CNQD, there is no conductance gap with QD's size smaller than 7 layers, and the conductance peak around the interface quasilocalized state −0.26 eV disappears with QD sizes larger than 23 layers. In addition, for the (5,5)/(10,0)/(5,5) CNQD, the connection method can change the degree of electronic localization of intermediate (10,0) tube.

PACS. 61.48.+c Fullerenes and fullerene-related materials – 71.20.Tx Fullerenes and related materials; intercalation compounds – 72.80.Rj Fullerenes and related materials – 68.55.Ln Defects and impurities: doping, implantation, distribution, concentration, etc.

1 Introduction

The continual miniaturization of electronic devices has always been a major driving force in the microelectronic industry. The ultimate goal is to synthesize devices as small as possible, i.e. as small as a molecule or a cluster of atoms. Molecularly perfect materials such as single-wall carbon nanotubes (SWCNs) can provide new opportunities for designing nanometer-sized electronic devices.

SWCN can be either metallic or semiconducting depending on both the diameter and chirality, which can be uniquely determined by the chiral vector (n,m), where n and m are integers [1]. If two nanotubes (one semiconducting and the other metallic) are connected, a heterojunction is formed which can act as a rectifying diode. Such two-terminal heterojunctions or rectifying diodes were first postulated theoretically [2], and recently observed in experiments [3,4]. Transport measurements performed in SWCNs, which were deposited on metallic contacts [5,6], have given evidences of resonant tunnelling through quantized energy levels. Such reports stimulated several theoretical models of CNQDs. Recently, carbon nanotube Y-junctions were produced by Li et al. [7], and theoretically studied by [8]. These tubular heterostructures called intramolecular heterojunctions (IMJs) offer new perspectives for nanoelectronic technology. Chico et al. [9] first proposed that a quantum dot can be obtained by combining two carbon-nanotube metal-semiconductor junctions, which behaves as an ideal zero-dimensional device. Both the discrete nature and the spatial localization of the (5,5) tube-derived states unambiguously demonstrate quantum confinement. Therefore, the (6,4)/(5,5)/(6,4) system behaves as a quantum dot, and is thus called a carbon nanotube quantum dot (CNQD). The singular electronic properties of CNQDs may be important in future nanoelectronics, since a CNQD with metallic contacts could behave as a one-electron transistor, and Coulomb blockade effects due to occupation of these strongly localized discrete levels are expected. So it could be envisioned to integrate an electronic circuit of nanotube based architecture, where multi-terminal junctions or nodes have multifunctional logic characteristics. However, the detailed

[a] e-mail: liuhong3@pine.njnu.edu.cn

calculation of electron transport phenomenon through IMJs which include the influences of structure and size are required.

In this work, we have performed calculations of the electronic structure and quantum conductance of the (10,0)/m(5,5)/(10,0) CNQD, which is different from the (6,4)/(5,5)/(6,4) QDs studied by Chico et al. [9]. The size dependence of the QD states is investigated, as required for the design of a quantum device. Furthermore, we studied another type of CNQD, namely M/S/M (5,5)/m(10,0)/(5,5), which has three different topological configurations. The section between two semi-infinite SWCNs can be considered as one quantum dot. We also studied their general quantum characteristics, together with the dependence of the number and localization of bound states on the size of QDs. We adopted a tight-binding Hamiltonian and followed the single-particle Green's function formalism to obtain LDOS within real-space renormalization techniques [10,11]. Given that electron transport on the molecular scale has become a topic of intense applications, we also calculated the conductance of CNQDs adopting the Landauer-Kubo formalism [12]. This work is organized as follows: in Section 2, we present the theoretical method. In Section 3, we proceed with the numerical calculations, and give discussions. Finally, the summary is given in Section 4.

2 Theoretical method

We perform the calculation of the local density of states (LDOS) and quantum conductance to characterize the electronic properties within a tight binding description of the carbon bonds. We use the following Hamiltonian

$$H = \sum_{\langle i,j\rangle,s} V_{pp\pi}\left(C^{+}_{i,s}C_{j,s} + C_{i,s}C^{+}_{j,s}\right), \tag{1}$$

where $\sum_{\langle i,j\rangle}$ is restricted to nearest-neighbor atoms, and $V_{pp\pi} = -2.75$ eV is the two-center hopping integral. On-site energies are set to zero, therefore the Fermi energy E_F is zero. All the hopping parameters are equal, independent of the bond length, curvature, or any rearrangement due to the presence of defects. Therefore, the changes are solely induced by the alterations in the topology of the hexagonal rolled lattice.

The metallic contacts are realized by two different carbon nanotube (CNs) in order to investigate their roles in the conductance. Electronic correlations are neglected in this simple calculation, although they are relevant for a proper description of confined systems such as the proposed quantum dots. Since we consider a real-space Hamiltonian, the details of the atomic arrangement of the junction may be completely incorporated through an adequate microscopic description. Surface Green's functions for the semi-infinite CNs are calculated through the solution of matrix-like Dyson equations obtained by successive decimations of unit cells. The average LDOS at ring j and energy E is given by $\rho_j(E) = -1/(\pi n_j)\mathrm{Im}\mathrm{Tr}G_{j,j}(E)$, where Tr stands for the trace over the n_j carbon atoms of ring j, and $G_{j,j}(E)$ refers to the Green's function at ring j. Let us consider a heterojunction C connected to two semi-infinite SWCNTs. The conductance is most conveniently solved using the Green's function matching (GFM) method. A fundamental result in the theory of electronic transport is that the conductance through a region of interacting electrons is related to the scattering properties of the region itself via the Landauer formula: $\mathcal{T} = (2e^2/h)T$, where $\mathcal{T}$ is the conductance, and T the transmission function is expressed as such

$$T = \mathrm{Tr}\left(\Gamma_L G^r_C \Gamma_R G^a_C\right). \tag{2}$$

$G^{r,a}_C$ represent the retarded and advanced Green's function of the heterojunction, respectively, and $\Gamma_{L,R}$ represents the couplings of the heterojunction to the left and right SWCNTs, respectively. The Green's function (G_C) as a function of energy E is defined as

$$G_C = (E - H_C - \Sigma_L - \Sigma_R)^{-1}, \tag{3}$$

where $\Sigma_{L,R}$ are the self-energy terms due to the semi-infinite SWCNTs, and H_C is the Hamiltonian of the heterojunction. The self-energy terms also define the coupling Γ through the following relation:

$$\Gamma_{L,R} = i\left[\Sigma^r_{L,R} - \Sigma^a_{L,R}\right]. \tag{4}$$

In turn, the self-energy terms are calculated with a previously published surface Green's function matching technique [13].

3 Results and discussion

First, we calculate the electronic properties and quantum conductance of a single (5,5)/(10,0) interface. To confirm the resonant behavior of the system, we plot both quantum conductance and the local density of electronic states (LDOS) together in Figure 1. The energy range of interest is from -0.45 eV to 0.45 eV around the semiconductor gap of the infinite (10,0) tube. The quantum conductance gap of the interface (5,5)/(10,0) is from -1.6 eV to 1.6 eV as determined by the (5,5) tube, which is larger than the band gap of the semiconducting segment (about 1 eV). The larger conductance gap is due to the mismatch in the conducting states of the (5,5) and (10,0) segments. The presence of 5–7 defect leads to a different LDOS for the conduction and valence bands. Even though one sharp peak in the LDOS for the (5,5)/(10,0) interface, is observed in the gap region, there is no peak in the gap region of quantum conductance. This shows that the interface quasilocalized states are off-resonance states. The basic characteristics of the LDOS and quantum conductance are in agreement with the results of Rochefort et al. [14], where they studied the quantum size effect of finite (5,5)/(10,0) junction between two gold leads using the

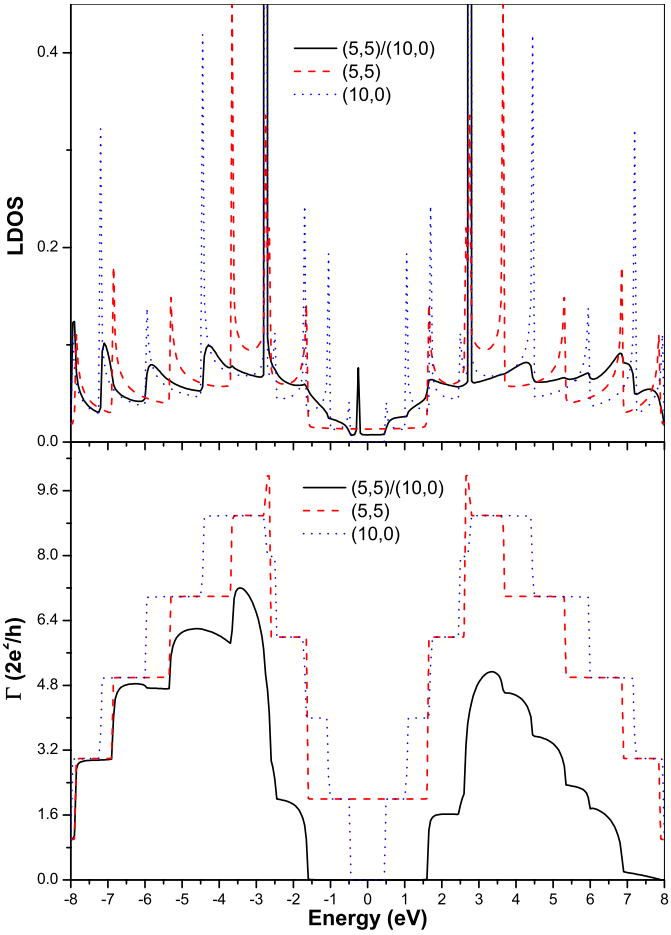

Fig. 1. The local density of electronic states and quantum conductance of single (5,5)/(10,0) junction.

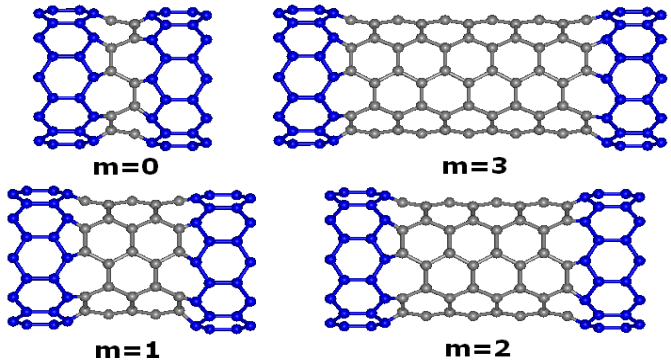

Fig. 2. Some structures of (10,0)/(5,5)/(10,0) QD with $3 \times m + 2$ layers.

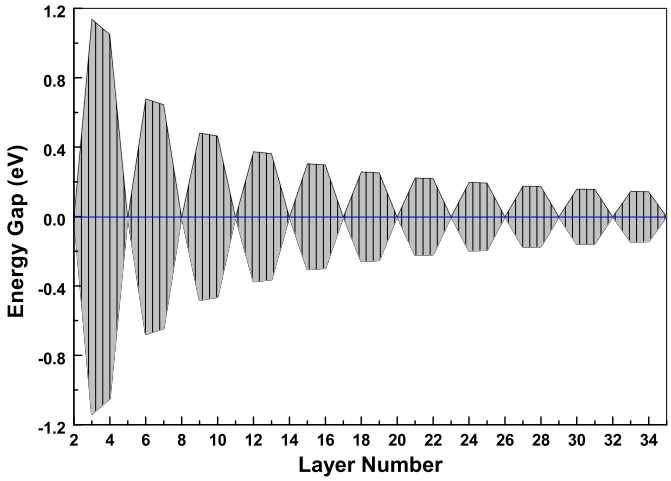

Fig. 3. The gap between HOMO and LUMO of individual finite (5,5) tubes with increasing lengths.

extended Huckel (EH) model. Next, let us study the quantum size effect of the quantum conductance and LDOS in CNQD for the two types of above-mentioned structures.

3.1 (10,0)/(5,5)/(10,0) CNQD

We now proceed to investigate the S/M/S (10,0)/(5,5)/(10,0) CNQD on the bases of the SWCN heterostuctures [15]. In Figure 2, the smallest intermediate (5,5) tube has only 20 atoms. The number of QD atoms is gradually increased to 350 using 10 atoms per layer. The first 10 atoms added to the QD are taken as layer a, and the second 10 atoms are taken as layer b. Contiguously adding two layers a and b corresponds to adding a unit cell to the (5,5) SWNT. The four special quantum-sized structures of the intermediate (5,5) QD are presented in Figure 2, in which three layers $a + b + a$ are added from 20 atoms to 110 atoms.

Before investigating the LDOS of the CNQD, we first show the electronic structure of individual tube (5,5) with different finite length. Through exact diagonalization of Hamiltonian, the relation of the gap between the highest occupied molecular orbital (HOMO) and lowest unoccupied molecular orbital (LUMO) of the (5,5) tube is plotted with increasing tube length in Figure 3. Physically, as we know, the band structure of armchair nanotubes consists of two non-degenerate bands which cross the Fermi level at $k = 2\pi/3a_0$, with lattice constant a_0. The wave vector k for finite tube samples is in units of $2\pi/L$, where L is the nanotube length. Clearly, only when $L = 3Na_0$ (with integer N) can one probe the Fermi level exactly where the two bands overlap. In Figure 3, we observe similar results. However, the peak at the Fermi energy $E_F = 0$ eV is only for sizes (called the fist type of size), which have $3 \times m + N_0$ layers with integer m, and $N_0 = 2$ meaning the unit cell for the (5,5) tube. For other quantum-sizes (called the second type of size), there is no peak at the Fermi level, which is also consistent with previous studies of the band gap for finite-length armchair nanotubes [16,17]. Furthermore, from Figure 3, it is found that with increasing the tube length becoming longer, the peaks simply crowd toward $E = 0$, and for the second type size its gap decreases.

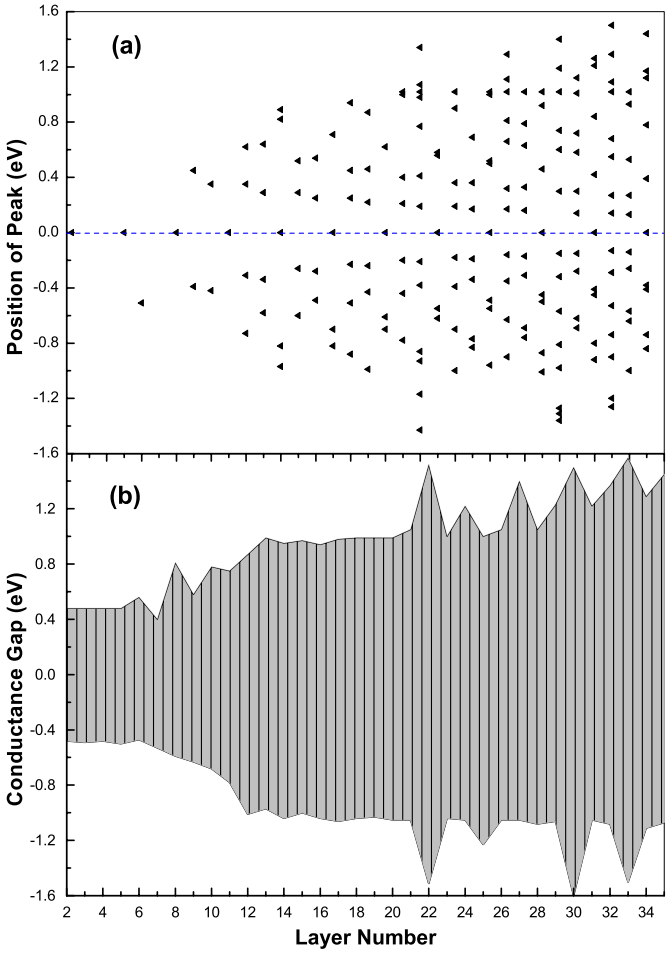

Fig. 4. The quantum conductance of (10,0)/m(5,5)/(10,0) CNQD with increasing size: (a) The changes of the peak positions in the conductance gap. (b) The variation of quantum conductance gap of (10,0)/(5,5)/(10,0) CNQD.

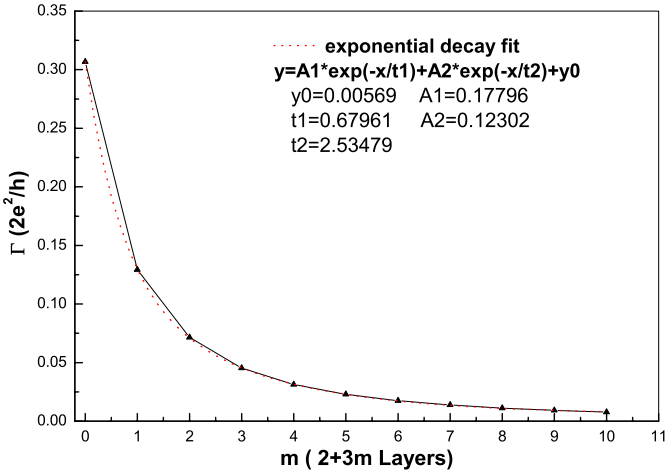

Fig. 5. The decrease in the height of the conductance peak at the Fermi energy of the (10,0)/(5,5)/(10,0) QD as a function of increasing size, and the second-order exponential decay fit to the height of peaks.

Next we carry out the calculation to study the dependence of the quantum conductance on quantum-size in this type of CNQD. We analyze the results of LDOS in CNQD with different sizes. The basic resonant characteristics of the CNQD have similar relation with size, i.e., only for the first type size is there a peak at the Fermi energy in the LDOS of CNQD. However, the results in (6,4)/(5,5)/(6,4) CNQD [9] did not show the characteristic that the resonant peak at the Fermi level periodically appears with increasing QD's size. Comparing the LDOS of CNQD with the energy levels of individual (5,5) tube, it is found that the positions of the peaks in LDOS of CNQD are not symmetric around $E = 0$ eV, which is due to the fact that topological defects break the electron-hole symmetry.

We now investigate the tunnelling peak in quantum conductance of the CNQD. In fact, two remarkable features are found in Figure 4: first, the number of peaks in the energy range of the (10,0) tube semiconductor gap varies with different sizes. With larger CNQD, the number of peaks gradually increases in this region. Furthermore, the resonant tunnelling peak at the Fermi energy in the conductance only occurs for the first type sizes shown in Figure 2. Second, the conductance gap of CNQD increases with increasing QD size. The first characteristic could be associated with the electronic properties of the (5,5) tube. As discussed above, the number of energy levels in the interesting energy region increase with increasing QD size. The series of quantum states stemming from energy levels of the (5,5) tube are intermingled, such that the states would manifest themselves as a resonance. The second characteristic can be understood by considering that the number of discrete states increases with increasing tube length. The number of the resonant states originating from intermingling between the discrete states stemming from energy levels of two (5,5) tube and (10,0) tube obviously increases and approaches the number of resonant states of the (5,5)/(10,0) junction. From Figure 4, one can see that even for very large size, the gap width still has certain features; namely the oscillation varies with the thickness of layer, and the gap width tends to the constant value of 3.2 eV when the QD's size is larger than about 30 layers.

In Figure 5, it is shown that the quantum conductance peak at the Fermi energy decreases exponentially with increasing number of layers (30 atoms per layer). The limiting value of the decay of the peak at Fermi energy is $5.69 \times 10^{-2}(2e^2/h)$. The CNQDs with the first type quantum-size are on-resonance devices at the Fermi energy.

Following to the discussion above, it is possible that the number and positions of the resonant peaks in conductance gap may be obtained from the electronic structure of the individual intermediate (5,5) tubes. The quantum conductance of CNQD with larger size is illustrated in Figure 6. It is found that in the conductance gap, the peaks

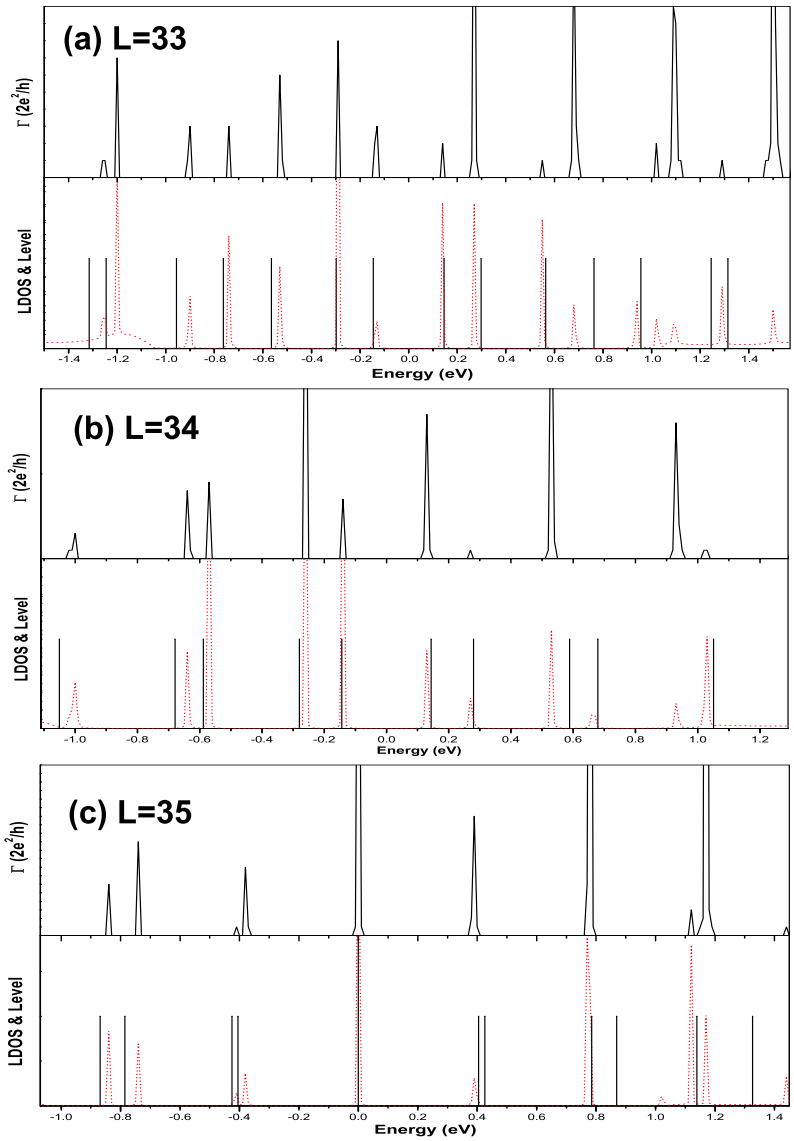

Fig. 6. The quantum conductance and LDOS of (10,0)/(5,5)/(10,0) CNQD, as well as the energy level of individual finite (5,5) tube with various sizes: (a) layers = 33, (b) layers = 34, (c) layers = 35. The dotted lines are LDOS and the vertical solid lines are energy levels.

around the Fermi energy nearly correspond to the relative energy levels, and those far from the Fermi energy deviate a little from the relative energy levels. This is obvious in the case of larger sizes. In addition, with longer tube, the distribution of energy levels are more uniform, and thus the resonant peaks are distributed more uniformly in the conductance gap, which is in agreement with the results by Chico et al. [9].

3.2 (5,5)/(10,0)/(5,5) CNQD

We also proceed with the same numerical scheme for M/S/M (5,5)/m(10,0)/(5,5) CNQDs, in which the (10,0) tube has three methods of being connected to two semi-infinite (5,5) tube leads as shown in Figure 7. The number of the CNQD atoms can be gradually added up to about 600 (40 atoms per layer). Among the three types of (5,5)/m(10,0)/(5,5) CNQD, the structures (a) and (b) have the same layers but different symmetry, and the

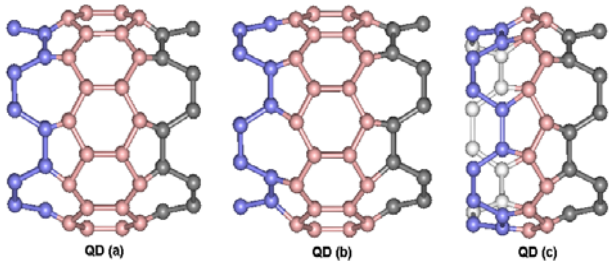

Fig. 7. The three types of (10,0)/(5,5)/(10,0) QD of smallest size, defined as QD (a), QD (b) and QD (c), respectively.

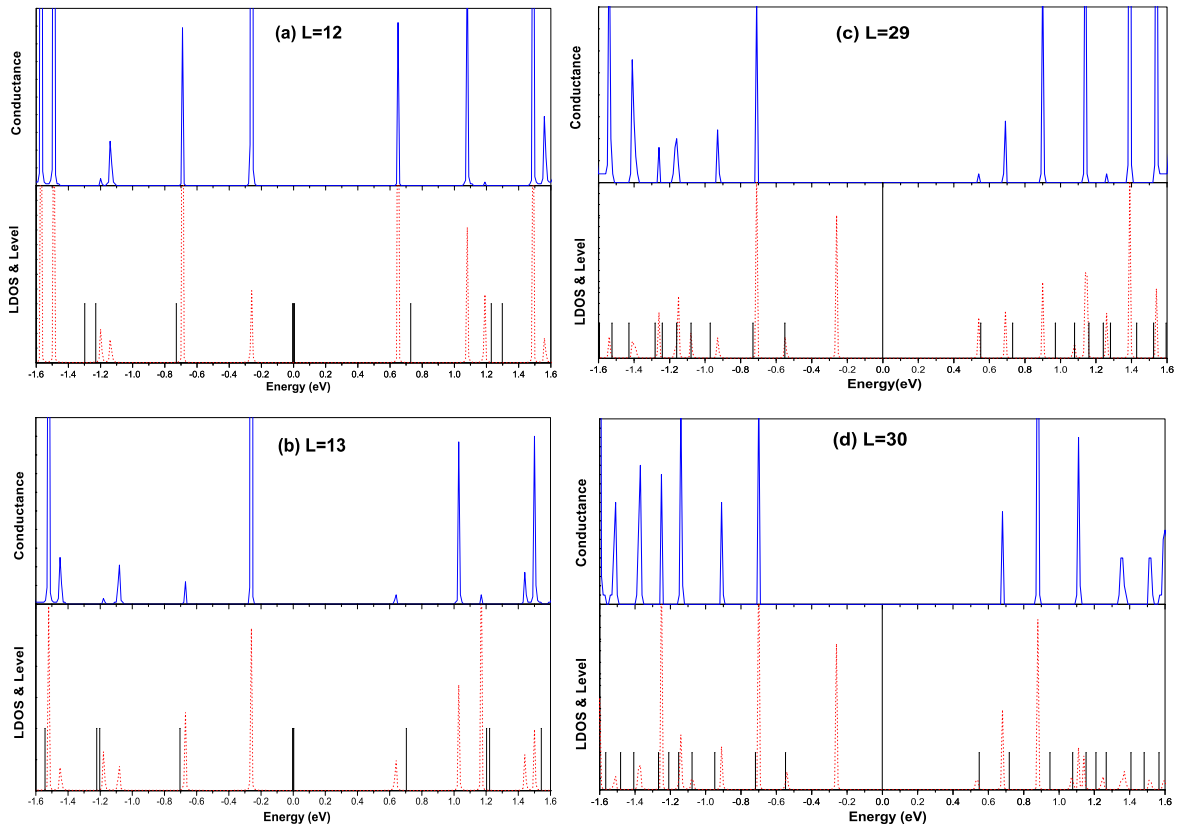

Fig. 8. The quantum conductance and LDOS of (5,5)/(10,0)/(5,5) CNQD, as well as the energy levels of the individual finite (10,0) tubes with various sizes: (a) layers = 12, (b) layers = 13, (c) layers = 29, (d) layers = 30. The dotted lines are LDOS and the vertical solid lines are energy levels.

structure (c) has a different number of atoms to the former two structures. If the cell with 20 atoms is taken as one layer, the structures (a) and (b) have an even number of layers, while the structure (c) has an odd number of layers. It is well known that the band structure of semiconductor zigzag nanotubes consists of a semiconductor gap around the Fermi level for all wave vector k points. However, for the finite (10,0) tube, the dangling covalent π bonds at the ends of the finite (10,0) tubes give rise to edge states at $E_F = 0$ eV, which have at least two degeneracies, and are different from the electronic properties of finite (5,5) tubes. With increasing tube length, the energy levels gradually tend towards $E = 0$ eV. Only when the finite (10,0) tube is rolled up into one ring without any dangling bonds, do the edge states disappear. Therefore the (5,5)/(10,0)/(5,5) CNQD will take on very different resonant characteristics.

In Figure 8 we give the LDOS in the energy range of interest from -1.6 eV to 1.6 eV for different sizes. It is shown that there is no peak at the Fermi energy for any size, which is different from that of (10,0)/(5,5)/(10,0) CNQD. We also notice two features in the LDOS: First, for CNQD(a) and CNQD(b) the peak positions and the number of these localized QD states are nearly the same as each others in the energy range -1.6 eV to 1.6 eV, and the difference among them is only the peak height. However, QD(c) has one layer less than the two former, and it has a different number of localized states and different peak positions.Second, one resonant peak around -0.26 eV always exists in the LDOS for all types of the CNQD of any size. This is due to the fact that the peak is the first one around Fermi energy and the highest among these peaks in their conductance gap. In addition, we find that for the LDOS of (5,5)/(10,0)junction shown in Figure 1, the position of the localized interface state of the junction is consistently around -0.26 eV. So this localized QD states of (5,5)/(10,0)/(5,5) CNQD is mainly due to the interface state of junction.

Next let us study the quantum size effect of the CNQD. Comparing quantum conductances with LDOS, one notices two remarkable features in Figures 8 and 9. First, with small sizes, there are simultaneous conductance peaks at the peak positions of localized QD states in the conductance gap, which are on-resonance. However, with size larger than 23 layers, the conductance peak at -0.26 eV disappears, therefore the localized state at -0.26 eV is off-resonance. For other localized states in the LDOS, the resonance feature is more obvious for larger QD. Second, compared with (10,0)/(5,5)/(10,0) CNQD, this CNQD has no conductance gap when the QD's size is smaller than about 7 layers (20 atoms in one layer), which must been taken into account in designing electronic devices. With increasing size, the width of the conductance gap and the number of resonance peaks in the gap both

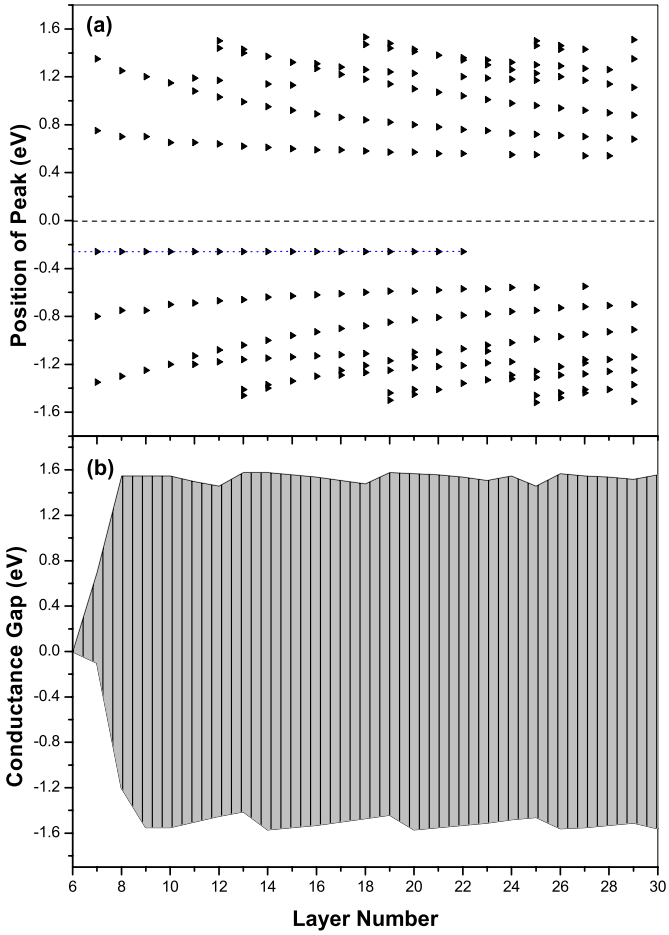

Fig. 9. The quantum conductance of (5,5)/(10,0)/(5,5) CNQD with increasing of size: (a) The changes of the peak positions in the conductance gap, (b) The variation of the quantum conductance gap of (10,0)/(5,5)/(10,0) CNQD.

gradually increase as shown in Figure 9. The width of the conductance gap slightly oscillates with size, and the maximal width of gap is about 3.2 eV. Even though the intermediate part of the CNQD is a semiconductor SWCNT, the (5,5)/(10,0)/(5,5) system behaves like a quantum dot. In the LDOS of the CNQDs (a), (b) and (c), with increasing QD size, the localized states gradually tend towards $E = 0$. Also the width between the two localized states around the Fermi energy gradually approaches the limiting value of about 0.90 eV, which is the semiconductor gap of the (10,0) tube.

Using the same procedure as for (10,0)/(5,5)/(10,0) CNQD, we analyze the possibility that the number and position of the resonance peaks in conductance gap may be obtained from the electronic structure of the individual intermediate (10,0) tube. In Figure 8 we found that in the conductance gap, the peaks around the Fermi energy almost correspond to the energy levels except for the interface state at -0.26 eV and the Fermi level, but for those peaks far from the Fermi energy, the correspondence is difficult. The feature is more obvious for larger sizes.

Finally, we analyze the influences of different connection methods on electronic properties of the CNQD. For CNQDs (a) and (b) with the same size, the positions of all the peaks are same, but the relative heights of peaks are different. Since the peak height corresponds to the squared amplitude of the wave function, a higher peak corresponds to the stronger degree of localization of localized QD state. Therefore the connection method can change the degree of electronic localization of the intermediate (10,0) tube.

4 Conclusion

The quantum conductance of two kinds of carbon nanotube quantum dot (CNQD) composed of (5,5) and (10,0) tubes, (10,0)/(5,5)/(10,0) and (5,5)/(10,0)/(5,5), are calculated for different quantum sizes. It is shown that one on-resonance peak at the Fermi energy of (10,0)/(5,5)/(10,0) QD exists only for special QD sizes. The conductance gap increases with increasing size, up to 3.2 eV. The positions of conductance peaks around Fermi energy and the number of conductance peaks in conductance gap can be obtained by the electronic structure of individual finite (5,5) tubes.

We also find that the (5,5)/(10,0)/(5,5) CNQD behaves as a quantum dot. Its localized QD states are different from that of the former due to the existence of the interface state in the (5,5)/(10,0) junction. There is no conductance gap when the QD size is less than 7 layers. The conductance gap width oscillates slightly with size, and the maximal width of gap is about 3.2 eV. There is one conductance peak around the interface quasilocalized state at -0.26 eV when size is smaller than 23 layers. In the conductance gap, the positions of conductance peaks around the Fermi energy can also be given by the electronic structure of individual finite (5,5) tube, however, the positions and the number of other conductance peaks far away the Fermi energy can not be evaluated from the energy levels. The connection method can change the degree of electronic localization of intermediate (10,0) tubes.

We thank Prof. Weicheng Huang for his contributions to the later discussion about this work.

References

1. R. Saito, M. Fujita, G. Dresselhaus, M.S. Dresselhaus, Phys. Rev. B **46**, 1804 (1992)
2. L. Chico, V.H. Crespi, L.X. Benedict, S.G. Louie, M.L. Cohen, Phys. Rev. Lett. **76**, 971 (1996)
3. J. Han, M.P. Anantram, R. Jaffe, J. Kong, H. Dai, Phys. Rev. B **57**, 14983 (1998)
4. Z. Yao, H.W.C. Postma, L. Balants, C. Dekker, Nature (London) **402**, 273 (1999)
5. S.J. Tans, M.H. Devoret, H. Dai, A. Thess, R.E. Smalley, L.J. Geerligs, C. dekker, Nature **386**, 474 (1997)

6. D.H. Cohen, M. Bockrath, N.G. Chopra, A. Zettl, P.L. McEuen, A. Rinzler, A. Thess, R.E. Smalley, Physica B **251**, 132 (1998)
7. J. Li, C. Papadopoulos, A. Rakitin, J. Xu, Nature (London) **402**, 253 (1999)
8. A.N. Andriotis, M. Menon, D. Srivastava, L. Chernozatonskii, Phys. Rev. Lett. **87**, 066802 (2001)
9. L. Chico, M.P. Lopez Sancho, M.C. Munoz, Phys. Rev. Lett. **81**, 1278 (1998)
10. M.B. Nardelli, Phys. Rev. B **60**, 7828 (1999)
11. M.S. Ferreira, T.G. Dargam, R.B. Muniz, A. Latge, Phys. Rev. B **62**, 16040 (2000); M.S. Ferreira, T.G. Dargam, R.B. Muniz, A.Latge, Phys. Rev. B **63**, 245111 (2001)
12. R. Kubo, J. Phys. Soc. Jpn **12**, 570 (1957)
13. M. Buongiorno Nardelli, Phys. Rev. B **60**, 7828 (1999); M. Buongiorno Nardelli, J. Bernholc, Phys. Rev. B **60**, 16338 (1999)
14. A. Rochefort, P. Avouris, Nano Lett. **2**, 253 (2002)
15. H. Liu, J. Chen, Acta Physica Sinica **52**, 664 (2003)
16. H.Y. Zhu, D.J. Klein, T.G. Schmaltz, A. Rubio, N.H. March, J. Phys. Chem. Solids **59**, 417 (1998)
17. A. Rochefort, D.R. Salahub, Ph. Avouris, J. Phys. Chem. B **103**, 641 (1999)